



Advanced receptor modeling of near–real–time, ambient PM_{2.5} and its associated components collected at an urban–industrial site in Toronto, Ontario

Uwayemi M. Sofowote¹, Ankit K. Rastogi², Jerzy Debosz¹, Philip K. Hopke³

¹ Air Quality Assessment and Reporting Unit, Environmental Monitoring and Reporting Branch, Ontario Ministry of the Environment, Etobicoke ON, M9P 3V6, Canada

² Faculty of Medicine, University of Toronto, Toronto ON, M5S 1A8, Canada

³ Institute for a Sustainable Environment, Clarkson University, PO. Box 5708, Potsdam NY, 13699–5708, USA

ABSTRACT

PM_{2.5} and other atmospheric pollutants were continuously monitored at high time resolution for 1 year at an urban–industrial location in Toronto, ON, Canada’s largest city. The data collected for these pollutants were examined to determine seasonal trends and potential sources. Advanced receptor models including residence time weighted concentration (RTWC) and simplified quantitative transport bias analysis (sQTBA) trajectory ensemble models (TEM) and conditional probability function (CPF) were applied to these data to identify potential local and regional sources of pollution impacting this receptor site. Seasonal trends showed that concentrations of PM_{2.5} were more frequently high in winter than in any other season. Median concentrations of lead and arsenic were highest in fall while median levels of chromium were not significantly different over the four seasons. The black carbon–derived measurement commonly known as Delta C (i.e., BC_{370nm}–BC_{880nm}) had its greatest abundance in winter and lowest levels in summer. The seasonality of Delta C is indicative of the impact of residential wood combustion near the receptor site. CPF indicated that lead and iron had the most unidirectional radial plots with sectors located west–southwest of the receptor being the most likely local source regions. Winter CPF for Delta C is almost of equal strengths in all directions suggestive of near–uniform isotropic local impacts. The sQTBA model provided the most satisfactory spatial representation of impacting sources. The strongest sources of PM_{2.5} identified by the sQTBA model were both local and transboundary in origin. More potential source regions were found in winter and summer than in spring and fall.

Keywords: PM_{2.5}, Delta C, Conditional Probability Function (CPF), Trajectory Ensemble Models (TEM), receptor modeling

doi: 10.5094/APR.2014.003



Corresponding Author:

Uwayemi M. Sofowote

☎ : +1-416-235-6186

☎ : +1-416-235-6037

✉ : Uwayemi.Sofowote@ontario.ca

Article History:

Received: 25 June 2013

Revised: 16 September 2013

Accepted: 22 September 2013

1. Introduction

Source apportionment of particulate matter (specifically fine PM; operationally defined as particles with aerodynamic diameter less than 2.5 μm, i.e., PM_{2.5}) in the ambient air has been an area of intense research over the past three decades (Thurston and Spengler, 1985; Ogulei et al., 2005; Ondov et al., 2006) due to the potentially negative health effects associated with particles and their constituent species (Pope et al., 2004). Specific toxic substances associated with PM could contribute to the overall PM health impacts (Harrison and Yin, 2000; Neuberger et al., 2004; Ondov et al., 2006). These substances include organic and inorganic contaminants including metallic species (Sunder Raman and Hopke, 2007) that may be helpful in tracing the sources of pollution. In recent years, receptor modeling including advanced factor analyses (Hwang and Hopke, 2007) and chemical mass balance approaches (Rizzo and Scheff, 2007; Dabek–Zlotorzynska et al., 2011) have been applied to the speciation of PM_{2.5} for the identification of the underlying source characteristics (factor profiles and contributions) impacting a given receptor site. Particulate matter in atmospheric samples collected at many urban locations may arise from direct emissions or secondary chemical processes from multiple contributory sources that could be natural or anthropogenic, situated locally or impacting the site via long–range atmospheric transport and deposition. Thus, the

interaction of the impacting sources of pollution will affect the nature, size and chemical composition of the particulates.

As part of its regulatory duties, the Ontario Ministry of the Environment (OMOE) maintains a province–wide ambient air monitoring network with real–time monitoring of specific contaminant species. Thus, PM_{2.5} is monitored at forty air quality stations and one research site in the province on a semi–continuous hourly basis. This high time resolution monitoring allows the Ministry to make timely assessments of air quality within the province. Though ideal, the use of near–real–time continuous PM_{2.5} data for source apportionment is generally limited to relatively short term campaigns spanning days to weeks (Jeong et al., 2004; Zhou et al., 2004b; Begum et al., 2005) due to instrumental and logistical constraints. Ogulei et al. (2005) used multiple time resolved species including near–real–time aerosol constituents collected over 9 months to identify up to nine sources of particulate matter pollution using advanced factor analyses. Hourly PM_{2.5} and its carbonaceous components were used to apportion the sources of Delta C and identify up to 8 factors of particulate matter pollution in recent multiple year studies (Wang et al., 2011; Wang et al., 2012).

Air quality in southern Ontario has historically been observed to be affected by long–range transport of pollutants from trans-

boundary source regions in the United States of America (Yap et al., 2005; Jeong et al., 2011). The mean annual composite PM_{2.5} concentrations measured in Ontario have been decreasing since 2003 (Ontario Ministry of the Environment, 2012). To manage the remaining sources, it is critical to assess the fine particle sources and differentiate between local and regional sources affecting the large metropolitan areas in Ontario. To this end, receptor modeling techniques were applied to semi-continuous ambient PM_{2.5} data collected for a year at a representative urban-industrial location adjacent to a sizable residential population.

This ambient data permit the assessment of seasonal trends of PM_{2.5} and selected carbonaceous and toxic metal constituents. Our main objective was to identify the sources of particulate matter pollution with the use of conditional probability-based receptor methods (CPF) for surface winds and more advanced trajectory ensemble models (TEM) including the residence time weighted concentration (RTWC) and the simplified quantitative transport bias analysis (sQTBA) models. These approaches do not require the establishment of the arbitrary conditional probability criteria/threshold values for the identification of potential local and regional sources. Previously, daily ambient monitoring data primarily from background sites in Ontario had been subjected to receptor modeling using potential source contribution function (PSCF) methodology (Ashbaugh et al., 1985) to identify potential local and regional sources of air pollution impacting the receptor sites (Zeng and Hopke, 1989; Cheng et al., 1993b; Zeng and Hopke, 1994). This is first receptor modeling study to apply advanced TEM on a large, continuous near-real-time PM_{2.5} and constituents' data that spans the four seasons of a year in Canada.

2. Experimental Section

2.1. Air sampling

Air monitoring for this work was performed at the OMOE Etobicoke South research station (43° 37' N, 79° 31' W; Figure 1)

located in Etobicoke (population: ~600 000) which is a neighborhood in metropolitan Toronto (population: ~2.5 million), the largest city in Canada. This area is industrialized with many small factories, industrial plants, and commercial facilities. Vehicular traffic is substantial due to the proximity of two major highways and traffic routes. Residential dwellings are located about 1 km west, south and east of the sampling site.

2.2. Instrumentation and quality assurance

The OMOE Etobicoke South research station is a temperature- and humidity-controlled shelter outfitted with a suite of real-time continuous ambient analyzers for PM_{2.5}, organic carbon (OC), elemental carbon (EC), black carbon and inorganic species including trace metals among other instruments. The instruments at the OMOE Etobicoke South research station are all continuous analyzers fitted with PM_{2.5} size inlets consisting of either stand-alone PM_{2.5} sharp-cut cyclones or PM₁₀ impactors coupled to PM_{2.5} cyclones. Unless otherwise stated, the inlets are operated at an air volumetric flow rate of 1 m³ h⁻¹. These inlets are located 2 m above the roof of the station shelter (3 m above ground level). Method detection limits and other data statistics of the analytes can be found in Table 1.

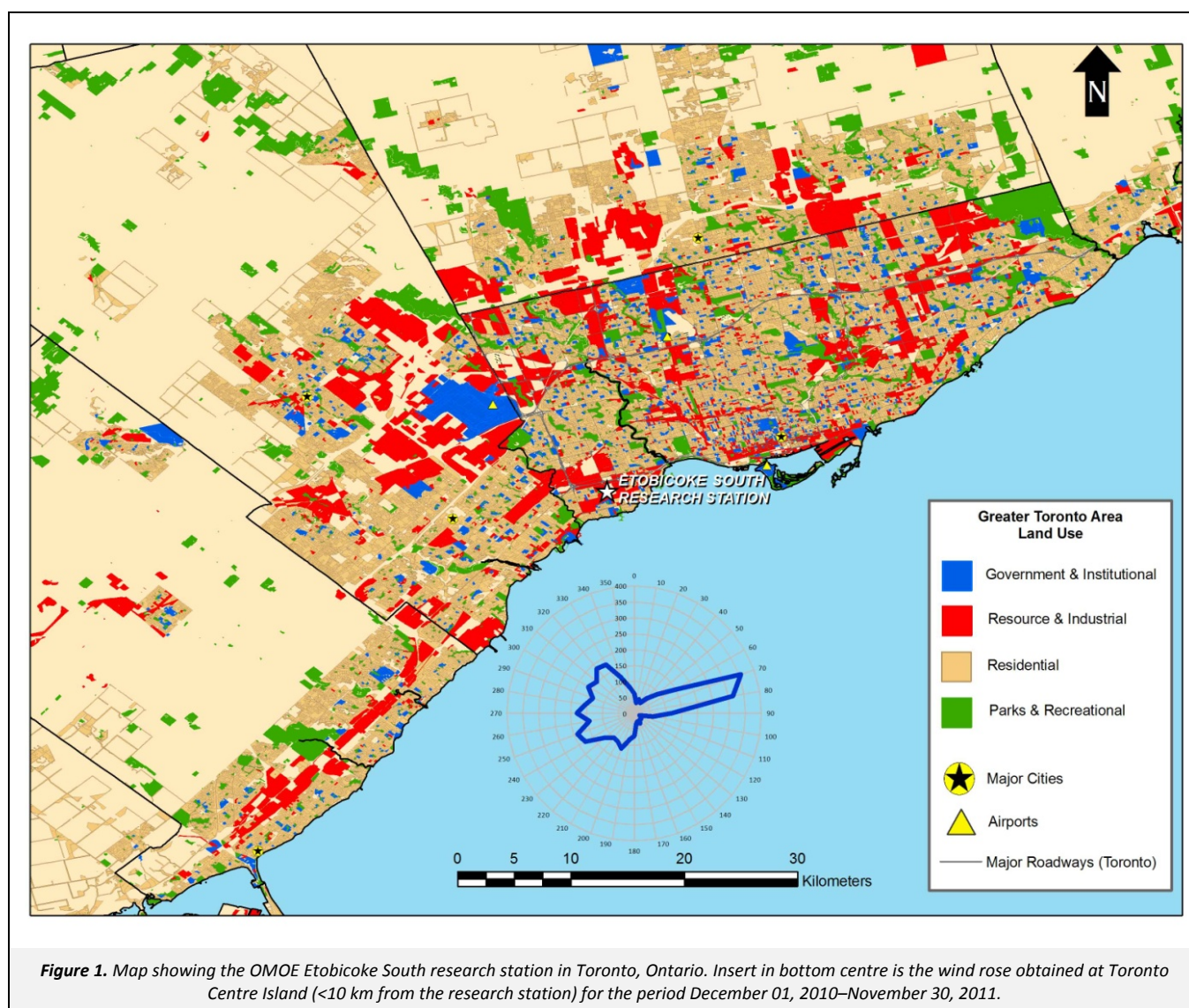
Near-real-time PM_{2.5} was determined at the research station with a Thermo Synchronized Hybrid Ambient Real-time Particulate (SHARP 5030, Thermo Fisher Scientific, Massachusetts, USA) monitor, a USEPA Class III Federal Equivalent Method (FEM) analyzer (U.S. EPA, 2011). The SHARP exploits the ability of aerosols to attenuate beta radiation and scatter light (nephelometry). Concentrations were calculated continuously in 60 minute cycles. Accuracy of measurement was within ±5% of 24 h Federal Reference Method and hourly precision at particulate concentrations less than 80 µg m⁻³ was ±2 µg m⁻³. Zero air calibration and glass fiber filter tape change were performed every 8–9 months (Thermo Fisher Scientific Inc., 2007).

Table 1. Summary of concentration data for nineteen pollutant species (see Section 2.2) collected as two-hour samples at the OMOE Etobicoke South research station for the period of December 01, 2010–November 30, 2011. A total of 4 380 two-hour samples was expected for the entire study period. The second column indicates the percentage of the total expected number of samples for which actual measurements were made. The third column indicates the percentage of the total expected number of samples with measurements greater than the method detection limit for each pollutant

Species	Data Available (%)	Data>MDL ^a (%)	MDL (×10 ⁻³ µg m ⁻³)	Median (µg m ⁻³)	Maximum (µg m ⁻³)	Minimum (×10 ⁻³ µg m ⁻³)
PM _{2.5}	95.2	93.6	500	8.00	61.5	ND ^b
OC	93.8	93.8	300	3.39	13.4	719
EC	93.0	63.3	300	0.495	7.32	ND
K	95.5	92.3	0.287	0.0271	6.94	0.00600
Ca	95.5	95.5	0.113	0.0540	2.20	ND
Ti	95.5	95.2	0.0630	0.00200	0.0889	0.0100
V	95.5	56.3	0.0480	0.000106	0.00995	0.00400
Cr	95.5	82.7	0.0390	0.000242	0.0393	0.00100
Mn	95.5	95.3	0.0240	0.00182	0.0626	0.00800
Fe	95.5	95.5	0.0280	0.0768	2.76	0.414
Ni	95.5	93.7	0.0130	0.000214	0.110	0.00100
Cu	95.5	95.5	0.0230	0.00309	0.216	0.128
Zn	95.5	95.5	0.0150	0.0113	0.423	0.195
As	95.5	84.9	0.0100	0.000424	0.0210	0.00100
Se	95.5	83.5	0.0110	0.000308	0.0275	0.00100
Br	95.5	94.9	0.0110	0.00256	0.0328	ND
Sn	95.5	60.0	0.899	0.00227	0.0414	0.01600
Ba	95.5	86.0	0.140	0.00188	0.440	0.00100
Pb	95.5	95.3	0.0190	0.00236	0.304	0.00800

^a MDL=Method detection limit.

^b ND=Non-detected. This symbol has been used to replace nominal zero values which were initially generated in the data logs.



Near-real-time analyses of metals were performed with a Xact™ 620 (Cooper Environmental Systems, Oregon, USA) ambient metals monitor (AMM). The Xact™ 620 ambient metals monitor is an X-ray fluorescence (XRF) spectrometry system at ambient pressure. The system can measure up to the twenty-five elements mainly found in periods 4–6 of the periodic table (Ag, As, Ba, Br, Ca, Cd, Co, Cr, Cu, Fe, Hg, Ga, K, Mn, Mo, Ni, Pb, Pd, Sb, Se, Sn, Ti, Tl, V and Zn). A limitation of this system is that it cannot determine elements with atomic mass lower than potassium. Upon optimization, a two-hour sampling time was selected as the preferred averaging time for these elements based on observed ambient levels and the method detection limits.

The data in Table 1 includes concentration ranges for the 16 elements that were observed at least 50% of the sampling period. Ag, Cd, Co, Ga, Sb, Tl, were seen less than 15% of the time and Hg was measured only 27% of the time. Data for Mo and Pd were eliminated because of bias resulting from operational constraints (Mo materials make up integral parts of the XRF module and Pd is used to monitor overall performance within the instrument). Full recalibration of the XRF module was done every 8 months and monthly calibration checks were made in triplicate with authentic thin film standards traceable to the National Institute of Standards and Technology (NIST, Maryland, USA) for 6–8 elements. Accuracy was within $\pm 10\%$ of the reference values and the measurement precision was within $\pm 5\%$ (Cooper Environmental Services, 2009). Yadav et al. (2009) have demon-

strated that comparable or better sensitivity and detection limits are obtainable with the Xact™ 620 monitor when compared to established 24-h reference methods.

OC and EC are important constituents of particulate matter derived from combustion sources and atmospheric chemistry forming secondary organic aerosol. They were monitored in near-real-time with a Sunset Semi-Continuous OCEC Carbon Aerosol Analyzer (Sunset Laboratory Inc., Oregon, USA) fitted with a $PM_{2.5}$ sharp-cut cyclone and an organic denuder. The principles of operation, sensitivity, and precision of the Sunset OCEC analyzer have been described by Bauer et al. (2009).

Hourly Delta C measurements were made by calculating the difference between black carbon (BC) monitored at 370 nm and 880 nm (i.e., $BC_{370nm} - BC_{880nm}$) in a dual-wavelength Aethalometer (Model AE21, Magee Scientific Co., California, USA). Delta C (Allen et al., 2004; Wang et al., 2011) has been used as a tracer for wood combustion (Wang et al., 2012). The instrument operates continuously at a flow rate of $0.3 \text{ m}^3 \text{ h}^{-1}$ (at 20°C). Flow calibration is performed every six months and a complete instrumental check-up is performed every 2 years.

Hourly meteorological data comprising near-surface wind speed, wind direction, ambient temperature, pressure and relative humidity were obtained from the closest Environment Canada Weather Station (Environment Canada, 2013a) located at the

Toronto City Centre (<10 km). The dataset used in this work comprised high resolution samples of PM_{2.5} (hourly) and the selected elements (two-hour) collected between December 01, 2010, 00:00 h EST and November 30, 2011, 23:00 h EST. In all, a total of 8 760 hourly samples of PM_{2.5}, OC and EC and 4 380 two-hour samples of metals were expected. The percentages of data that was actually available and of samples of each pollutant with concentrations above their method detection limits are given in Table 1.

3. Receptor Modeling of the Pollutant Species

Receptor models were applied to ambient concentration data for PM_{2.5}, OC, EC, Delta C, Br and the other species in Table 1 at the OMOE Etobicoke South research station for the identification of potential source regions. RTWC and sQTBA use air mass back trajectories while conditional probability functions (CPF) uses surface wind directions. These receptor models are briefly discussed in the section below, more detailed discussions on the formulations and characteristics of these models can be found in the Supporting Material (SM) and the literature cited.

Seventy-two hour back trajectories in hourly intervals starting at the receptor site were computed using the National Oceanic and Atmospheric Administration's Hybrid Single-Particle Lagrangian Integrated Trajectory (HYSPLIT) model (Draxler and Rolph, 2010) with winds from the National Centers for Environmental Prediction (NCEP) Global Data Assimilation System (GDAS) database for the entire 1 year period of sampling. Three-day back trajectories were used in this work because they offer a good compromise between synoptic scale transport and positional errors. A compilation of trajectory uncertainties shows that the minimum absolute horizontal transport deviation (AHTD) of trajectories after 72 h of travel is in the order of ≥ 500 km (Stohl, 1998; Stohl and Seibert, 1998). Errors with the HYSPLIT model are 15–30% of the total travel distance (NOAA ARL, 2008). In general, ensemble methods such as the ones herein work best with sufficient data (as with multiple receptor sites) since they average out the random errors associated with trajectories.

Relevant trajectory outputs for this study included latitude-longitude coordinates and time segments of endpoints. In the current work, the HYSPLIT back trajectories were computed for 500 m a.g.l. arrival height and initiated every three hours each day. The 500 m arrival height in this study was deemed satisfactory since back trajectories arriving near the surface at the receptor site had mixing heights ranging from 70 m–1 200 m. Additionally, this height is still below the 700 m maximum limit recently recommended by Westgate and Wania, (2011) for trajectories used in source apportionment studies and is consistent with other studies (Begum et al., 2005; Jeong et al., 2011).

In all, over 1×10^5 back trajectory endpoints were used and all pollutant data were converted to a two-hour time base for uniformity. MetCor (Rastogi, 2013); a software package that computes TEM (Sofowote et al., 2011; Venier et al., 2012) was used to obtain results in $0.75^\circ \times 1^\circ$ (LAT-LON) grid cells which at latitudes of $\sim 40^\circ$ gives an approximate 80 km \times 80 km grid size. Visualization of the TEM outputs was done using ArcGIS 9.3 (ESRI, California, USA). Details of how MetCor and ArcGIS were used for this work are in the SM.

3.1. Conditional Probability Function (CPF)

Conditional probability models compute the likelihood that an air mass that reaches the receptor is laden with a high concentration of a given pollutant (Ashbaugh et al., 1985; Cheng et al., 1993a). The definition of "high concentration" is arbitrary and may be an over-simplification. Here, the 90th percentile of analyte concentrations was used as the criterion. CPF is an extension of the

potential source contribution function (PSCF) model for surface meteorological data collected at the sampling site. For a given air mass arriving at the receptor from a given wind sector characterized by the angle $\Delta\theta$, CPF is defined as:

$$CPF_{\Delta\theta} = m_{\Delta\theta} / n_{\Delta\theta} \quad (1)$$

where $n_{\Delta\theta}$ is the total number of times air masses arrive from sector $\Delta\theta$ (set at 10° in this study) and $m_{\Delta\theta}$ is the number of times the air masses that arrive from $\Delta\theta$ are greater than the pre-defined criterion/threshold value. For those wind sectors with few events (value less than one third of the average number of events per sector), the CPF value was downweighted by a factor of 0.5.

CPF is more suitable to the identification of local sources (Kim et al., 2003; Kim et al., 2005; Pekney et al., 2006) since it does not actually identify a specific geographic location but only gives the directions of potential sources.

3.2. Residence Time Weighted Concentrations (RTWC)

RTWC (Stohl, 1996) achieves an iterative modification of the concentration weighted trajectory (CWT) model (Seibert et al., 1994) by allowing the trajectory segments to be included in the summation terms of the CWT calculation. The objective was to improve concentration-based identifications of source regions by using the time spent over a potential source region (residence time) to discriminate between trajectories associated with low and high concentrations at the receptor site. More details on this model can be found in the supplementary information.

Savitzky-Golay smoothing (filter length=15-point, polynomial order=1, confidence interval=0.99) was applied between runs to remove insignificant values in the newly generated CWT fields and convergence was pre-specified as 10% difference between successive iterations.

3.3. Simplified Quantitative Transport Bias Analysis (sQTBA)

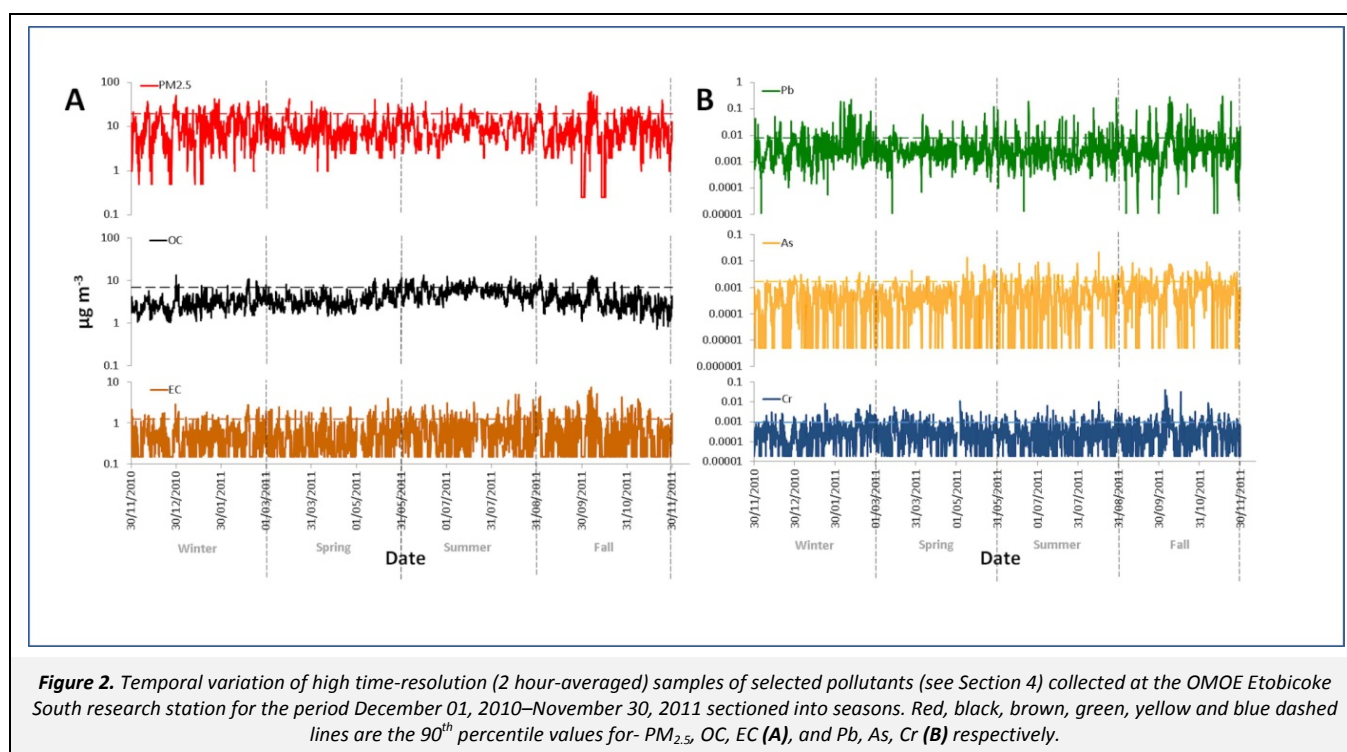
Other than the original work, QTBA (Keeler and Samson, 1989) has only been applied without the inclusion of chemical transformations and wet and dry deposition (Brook et al., 2004; Zhou et al., 2004a; Brereton and Johnson, 2012). The concentration-weighted transport potential fields were normalized by the natural transport potential fields to make the results less dependent on wind flow/trajectory patterns and improving the model's ability to identify potential source regions. It was further simplified by Zhao et al. (2007) who introduced a simple weighting scheme based on the average of the mean natural transport potential field so as to reduce tailing effects. More details on this model are given in the SM.

4. Results and Discussions

This work focuses on the trends and sources of PM_{2.5}, Delta C and three selected toxic elements (As, Cr and Pb) selected due to their potential toxicity (Goyer, 2004). The Xact AMM does not speciate the Cr which consists of the more abundant but non-toxic trivalent species and the carcinogenic hexavalent species. Data for the other pollutants have been included in the SM.

4.1. Seasonal trends

The 2-hour concentrations of PM_{2.5}, OC, EC, Cr, As and Pb for the entire period of study sectioned into seasons are shown in Figure 2 while Delta C is shown in Figure S5 (see the SM). Values below the method detection limits have been replaced with $\frac{1}{2}$ MDL for that species.



Temporal trends in the pollutant species were assessed graphically (Figure 2, Figures S1–S5, see the SM) and statistically (Tables S1–S4, see the SM). The data generally showed very low concentrations with episodic spikes and were not normally distributed. A non-parametric multiple comparison test was applied to the data to assess the seasonal variation of the pollutants of interest. Results of the Dunn's test after a Kruskal–Wallis non-parametric one-way analysis of variance (ANOVA) at $\alpha=0.05$ for the seasonal pollutant average concentrations can be found in Table S4 of the SM. All four seasons yielded statistically different mean ranks for most pollutants with the exception of Cr that was not significantly different among the seasons. Delta C was significantly higher in winter and significantly lower in summer while spring and fall mean ranks were not significantly different from each other.

Thus, for an alternative assessment of the data, the 90th percentile value was applied as the distinguishing threshold in the subsequent CPF computations. The selection of this threshold while arbitrary was made because at $20 \mu\text{g m}^{-3}$ for $PM_{2.5}$, it fell between the current annual U.S. National Ambient Air Quality Standard (NAAQS: $15 \mu\text{g m}^{-3}$) and the 24h Canada–Wide Standard (CWS: $30 \mu\text{g m}^{-3}$). The 90th percentile for each pollutant is shown as a dashed line in Figure 2 (see also Figures S1–S4 in the SM). Table 2 summarizes the number of times in each season that the 90th percentile was exceeded (see also Table S1 in the SM). In winter, $PM_{2.5}$ and Delta C had their highest number of exceedance. The greatest occurrence of As, Cr, Pb, and EC exceedance was in the fall while OC exceeded its 90th percentile the most in summer. The wintertime inter-quartile range (IQR) of Delta C is roughly 4 and 5 times the fall and spring IQR and is vastly greater than the summer IQR (see the SM, Table S3). This seasonal variation of Delta C may be indicative of impacts from local residential wood combustion during winter and is consistent with recent findings (Wang et al., 2011). Delta C has been shown to trace wood combustion (Wang et al., 2010) and could potentially differentiate diesel and wood combustion emissions (Wu et al., 2007; Wang et al., 2012). The scatter plots in Figures S6a–S6d (see the SM) show the seasonal variations in the Delta C– $PM_{2.5}$ relationship. Relationships of Delta C and other pollutant species such as K, EC and OC can be found in Figures S7–S11 (see the SM).

In winter (see the SM, Figure S6a), a ratio of 1:7.5 was obtained for the observed edge (Henry, 2003; Paatero et al., 2005) of the Delta C to $PM_{2.5}$ relationship. This ratio is identical to that observed in Rochester, NY in winter (Wang et al., 2011). The spring edge (see the SM, Figure S6b) is steeper indicating that up to 17% of the $PM_{2.5}$ mass in spring is related to wood smoke through the measured Delta C. The steepness of the edge is due to the highest point on the plot which corresponds to the Delta C observed for 04:00 h on May 10, 2011 (see the SM, Figure S5), the highest for the entire study period where it made up to 23% of the $PM_{2.5}$ levels. The potential impacts of wood combustion emissions to this particular sample can be ascertained by looking at the relative locations of wild fires (see the SM, Figure S72) and the back trajectories that terminate at the receptor site (see the SM, Figure S73). The maps show that the trajectories pass through a fire hotspot in Quebec. The relationships of Delta C with OC, EC and K show that in general, the edges are steeper in winter while the summertime edges are shallower indicating enrichment of Delta C during the cold months relative to these other species.

4.2. Potential short-range/local sources

The CPF plots in Figures 3a–3d were computed for the two-hour concentrations of $PM_{2.5}$, As, Cr, and Pb. Data obtained during periods of calm winds (surface wind speeds lower than 1 m s^{-1}) were observed 10.7% of the total period of study and were removed prior to CPF calculations. As seen from the local wind rose (lower middle insert in Figure 1), prevailing winds come from the west and are almost isotropic from the east with almost no winds from true north. CPF plots for the other species in this study are presented in Figures S12–S32 (see the SM).

The CPF plot for $PM_{2.5}$ (Figure 3a) indicated that the south–southwest sector may be the strongest source region followed by the southeast region. Potential local sources that lie in these directions include metals and chemical processing industries. Perhaps the clearest unidirectional CPFs were for Pb in (Figure 3b), Fe, Ti, and Mn (see the SM, Figures S12, S18–S19) indicating that the strongest source region lay in the west–southwest and south–southwest directions, respectively. Local metal processing industries in these directions are the likely sources. Cr (Figure 3c) seemed to be almost uniformly distributed from every direction,

but the strongest potential source region originated from the northeast direction. The emissions inventory map in Figure S35 (see the SM) shows that strong sources of Cr lie to the north-northeast relative to the Etobicoke receptor site. Although the use of lead chromate paints for line markings on roads was stopped in Ontario in January 2011 (Government of Canada, 2009), existing road markings may have been responsible for the near isotropic source of Cr in the other quadrants.

The CPF plot for As (Figure 3d) indicated the east sector where the Toronto harbor is situated and other areas in the southeast sector may be the strongest As source region. Arsenic emissions arise from combustion of coal and non-ferrous metals smelting and processing in addition to other area sources. There are no known/reported sources in the proximity of the receptor site

indicating that unknown local sources may be responsible for the observed directions. The CPF plot for vanadium (see the SM, Figure S15) also shows a strong easterly source presumably from oil-related emissions in Toronto harbor.

The seasonal CPF plots for Delta C are shown in Figures S28–S28D (see the SM). In winter, near-isotropic impacts can be observed except in the east-southeast quadrant where relatively stronger sources may be located. The extent of emitting sectors gradually diminishes after winter and show minima in summer where the south-southwest sectors are the major remaining source directions. In winter and spring (see the SM, Figures S28a and S28b), the strongest directions in the CPF plots clearly track the residential areas.

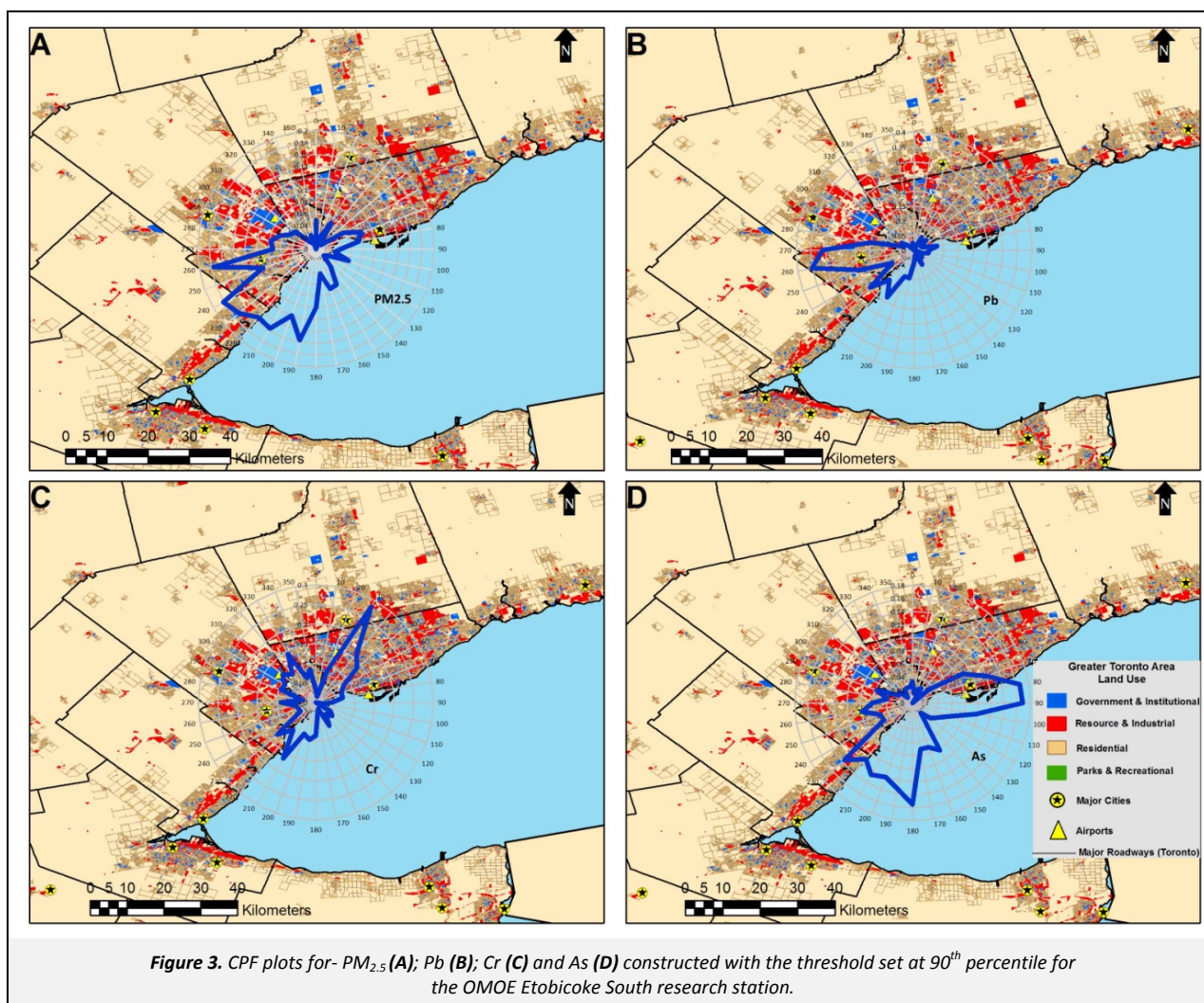


Table 2. Exceedance of the 90th percentile concentrations for selected pollutant species computed with 2 hour-averaged samples for the period of December 01, 2010–November 30, 2011. The 90th percentile concentrations for the pollutants are provided

Number of Samples Exceeding 90 th Percentile by Season	Species						
	$PM_{2.5}$	OC	EC	Delta C	Pb	Cr	As
Winter	156	27	57	248	126	95	44
Spring	64	47	84	53	66	96	71
Summer	64	254	125	11	82	86	105
Fall	107	85	139	85	144	143	200
Total Number of Samples Exceeding 90 th Percentile	391	413	405	397	418	420	420
90 th Percentile ($\mu g m^{-3}$)	19.5	6.89	1.26	0.129	0.00780	0.000969	0.0355

4.3. Comparisons of RTWC and sQTBA for PM_{2.5} and Pb

RTWC and sQTBA are trajectory ensemble models. These two models address different aspects of the source–receptor problem. Both RTWC and sQTBA were designed to be used with multiple site data so that there could be triangulation of the source locations. Here they are being applied to single site data and thus, may suffer from some of the same problems as PSCF.

Also, not all airborne pollutants in grids crossed by segments of the trajectory have equal probability of being transported to the receptor. Thus, sQTBA uses Gaussian distributions to calculate the natural transport potential function of a substance based on the distance and time interval away from the receptor.

The maps in Figure 4 show the RTWC and sQTBA fields for PM_{2.5} and Pb. In general, both models identified similar regional sources in most cases, but the strengths of potential sources vary between models. The RTWC is qualitatively less homogeneous due to the filtering and redistribution of concentration fields. These processes most severely affect grid cells around the receptor site. sQTBA has the added value of revealing local potential sources. The strength of local impacts at Etobicoke South arising from southern Ontario and the Great Lakes' coastal regions of New York, Pennsylvania and Ohio is seen. Because of the location of the receptor site in an urban area, industrial, residential, and vehicular sources significantly influence it. Furthermore, the county–level emissions inventory map of primary PM_{2.5} for parts of Ontario and

the US Midwest in Figure S33 (see the SM) suggest the potential contributions from local sources. The remaining discussion in this work focuses on results from sQTBA. RTWC source region maps for the remaining pollutants are in Figures S37–S53 in the SM.

4.4. Potential source regions from sQTBA of selected pollutants

Figure 5 shows source regions for As and Cr. Additional sQTBA maps for the other species in this work can be found in Figures S12–S26 (see the SM). These maps are quite detailed so only salient features will be discussed.

The map for PM_{2.5} (Figure 4a) indicates that in addition to local sources, strong potential sources could be as far removed from Etobicoke South as northern Alberta where petrogenic emissions may be potential sources for PM and trace species (Pb in Figure 4c and As in Figure 5b), the northern west coast of the USA and eastern Texas. Mid–continental USA shows many regions which may also be associated with high levels of PM_{2.5} at Etobicoke South. Relatively weaker impacts arise in northern and eastern Quebec and the mid–western states of Ohio, Pennsylvania, West Virginia, Michigan, Illinois and Missouri and as far out as southern Nevada and California. Interestingly, the Gulf of Mexico also gives rise to strong impacts. Begum et al. (2005) observed similar effects with PM_{2.5} and the sulfate component in the Gulf of Mexico which they discovered was attributed to the relatively high humidity in air masses arising in the Gulf. In general, more hotspots (strong source regions) can be found in the USA than in Canada. Examination of emissions inventories from Canada (Environment Canada, 2013b), and USA (U.S. EPA, 2013a; U.S. EPA, 2013b) show large primary emissions of PM_{2.5} in the identified regions.

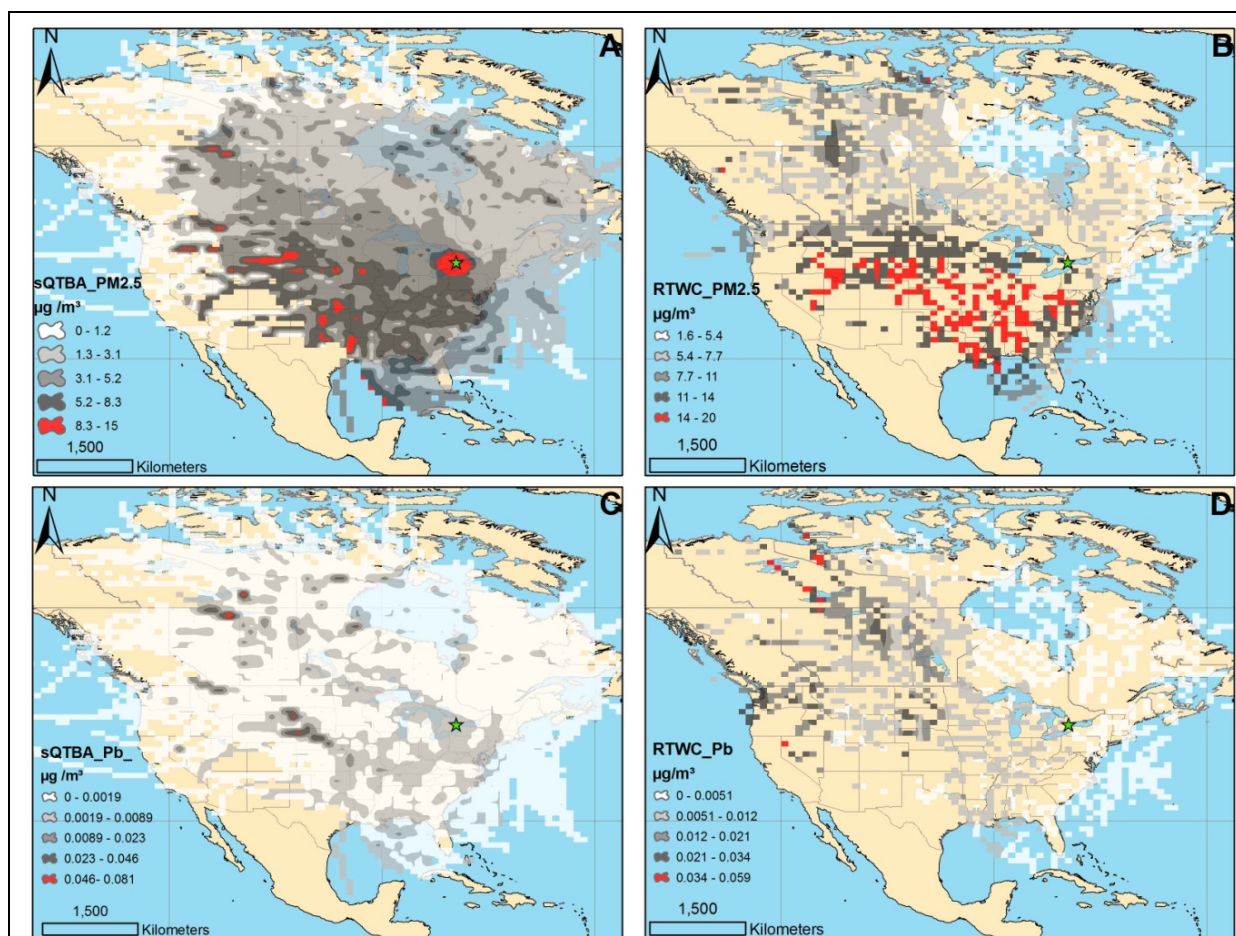
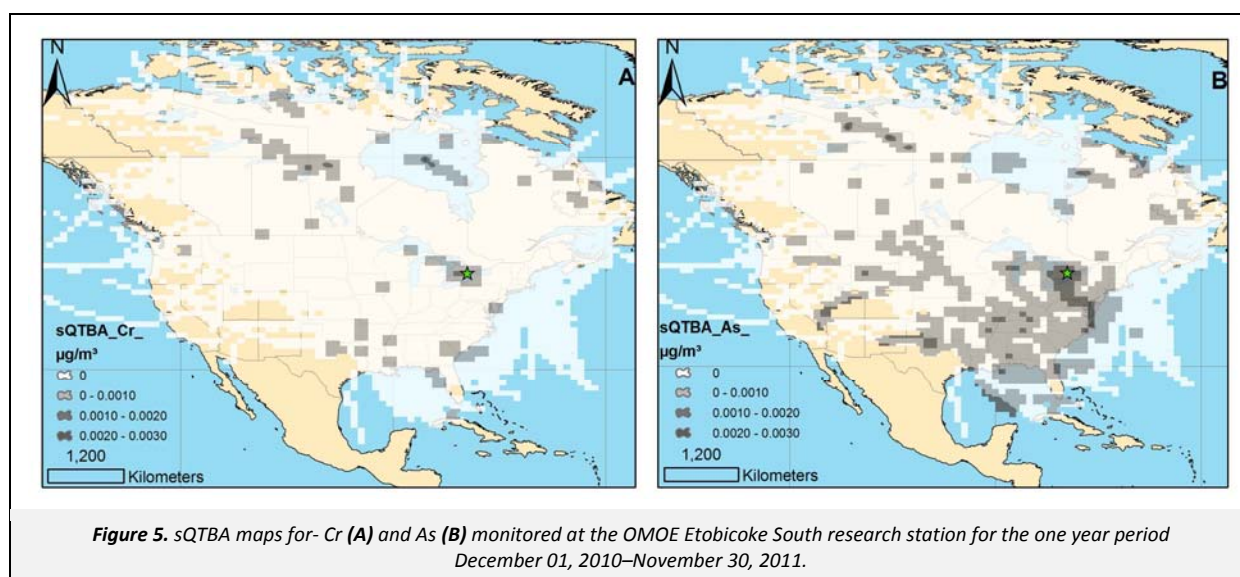


Figure 4. Comparisons of source regions identified by sQTBA (A-C) and RTWC (B-D) for PM_{2.5} and Pb monitored at the OMOE Etobicoke South research station for the entire one year period (December 01, 2010–November 30, 2011).



Based on the sQTBA map, lead (Pb, Figure 4c) has its strongest potential sources in areas well removed from the receptor site. Border regions of northern Alberta and the Northwest Territories were indicated as strong sources. Other strong hotspots can be found in South Dakota and Nebraska. Though the emissions inventory map does not explicitly reveal any major emitting county in this area, power generation plants can be found around these high potential regions, while in the Canadian north, mining and quarrying operations also can be observed. The sQTBA also indicated southern Missouri that includes the only primary lead smelter in the US (see the SM, Figure S34) as a potential source of lead to the Etobicoke receptor site. The hotspot in the lower Hudson Bay region of northern Manitoba warrants further investigation since it lies in a protected national park and may be due to trajectory positional errors. An electric power generating station and a non-ferrous metal production plant are situated about 200–250 km to its southwest.

There were not many Cr hotspots (Figure 5a) and they were mainly confined to southwestern Ontario. Two hotspots were identified in northern Manitoba. Power generation facilities in this area may help explain these hotspots.

The strongest potential sources of arsenic (As) traverse both sides of Lake Erie and extend to northern Virginia and New Jersey. Arsenic hotspots are also indicated in border regions of Missouri, Illinois and Kentucky and extend to the Gulf of Mexico in the southeast US and southern California, Nevada and Utah in the southwest (Figure 5b). These hotspots are at or near emitting sources (see the SM, Figure S36). Power generation, steel mills, primary metal production, and other manufacturing industries may be responsible for the high source strengths in these areas. In Canada, hotspots are seen in the border regions of the Northwest Territories and in northern Quebec where mining and smelter activities occur may help explain the As source in this area. The provincial, inter-provincial, and transboundary source regions indicated in the sQTBA maps of $PM_{2.5}$, Pb, As and Cr were compared to the national emissions inventories from Canada and the USA. The emissions inventory maps that were used for comparisons with the sQTBA maps in Figure 4 and 5 can be found in Figures S33–S36 (see the SM). These images indicate that the sQTBA results are reasonable.

4.5. Seasonal variations in the potential sources of $PM_{2.5}$

Seasonal sQTBA maps for $PM_{2.5}$ can be found respectively in Figure 6. Seasonal sQTBA maps for the other pollutants studied are in Figures S54–S71 in the SM.

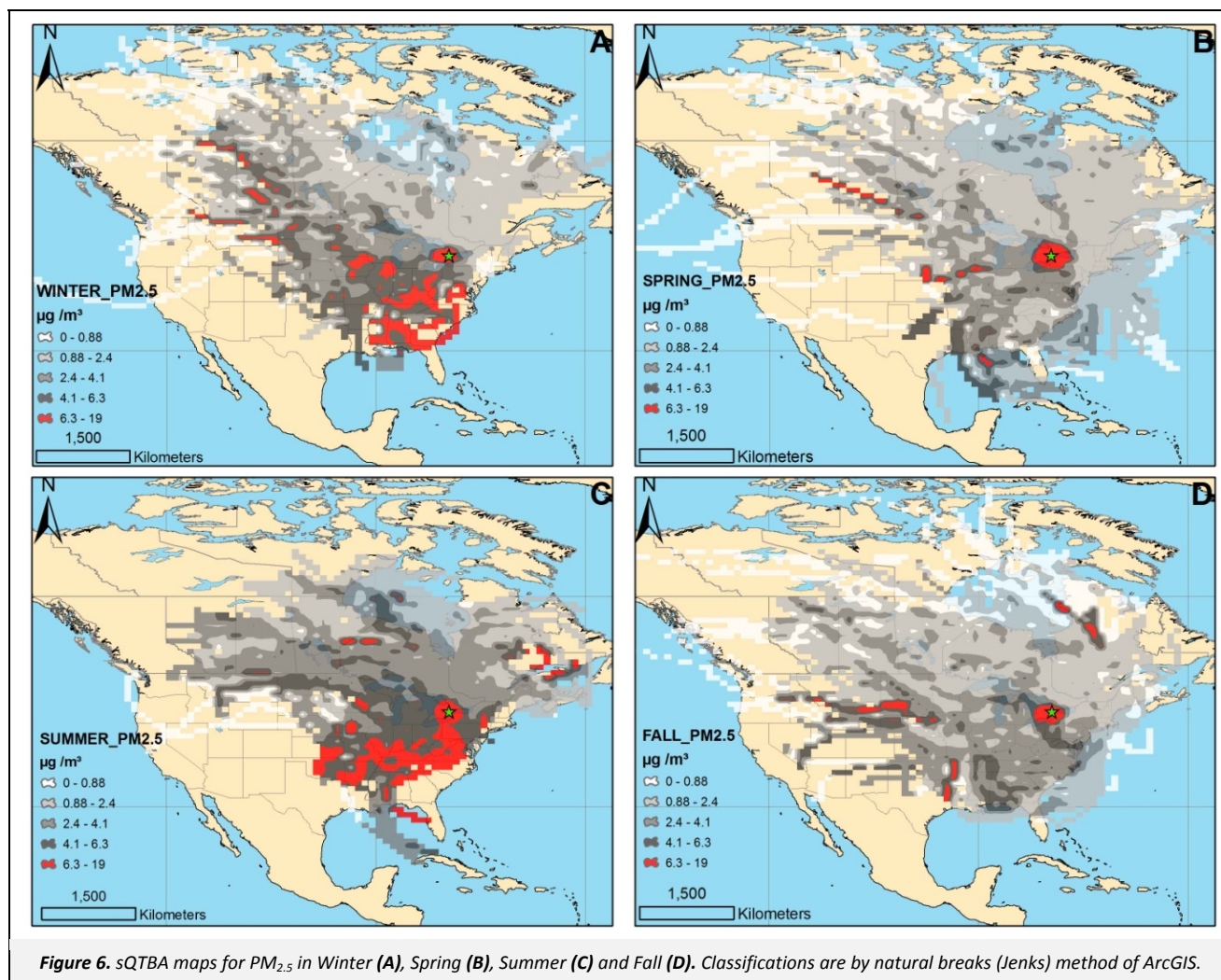
In general, local contributions of $PM_{2.5}$ can be observed all year round. There are more hotspots for $PM_{2.5}$ in winter than at any other time of the year and there is a greater spatial span of potential contributory regions. These factors may be responsible for the highest frequency the 90th percentile exceedance as noted in Table 2 above. In winter, hotspots of $PM_{2.5}$ have a markedly northwesterly and southerly flow relative to the Etobicoke South receptor site reaching as far as northern Alberta and southern coastal US states respectively. Winter and summer yield the greatest contributions from the US Midwest. It is clear that the Midwest is a major source region of $PM_{2.5}$ at Etobicoke South except in the spring. Interestingly, in the summer, hotspots can be found over clusters of industrial areas in Oklahoma and Kansas. In fall, northern Quebec may be a major source of $PM_{2.5}$ and hotspots as far as California and Nevada are observed.

5. Summary and Conclusions

Meteorologically based receptor models have been applied to a year's worth of ambient particulate data from a monitoring location in Toronto and examined the seasonal variation of the measured pollutant species. The highest fine particulate matter and Delta C concentrations were observed in winter while lead, chromium and arsenic had their high concentrations in the fall. The Delta C– $PM_{2.5}$ winter relationship is similar to other North American cities suggesting a similar source (residential wood combustion) for this carbonaceous species.

CPF plots for lead and iron strongly suggested local point sources of these pollutants probably due to metal processing plants which lie in these directions while the CPF plot for Delta C shows near isotropic impacts in winter that gradually reduced to a minimum in summer. Advanced trajectory models were used for receptor modeling of the ambient data. sQTBA consistently yielded more interpretable results than RTWC as the combination of redistribution and smoothing may have effectively removed all local sources. Comparison to national emissions inventories showed that anthropogenic activities were frequently observed in regions identified as hotspots of these pollutants.

Seasonal sQTBA maps revealed interesting features which could be helpful in understanding the sources and seasonal trends of the pollutant species. In winter, the latitudinal span of $PM_{2.5}$ hotspots is greater than at any other season. The strength of potential sources in the Canadian prairies was also greatest in winter. The U.S. Midwest is an important potential source region in the summer and winter sQTBA maps.



While normalization of the concentration-weighted transport potential fields by the natural transport potential fields reduces the effect of trajectory flow patterns in the source region identification, it is conceivable that it may still affect the sQTBA detailed herein since only one location was used. Thus, in future studies, we hope to be able to apply a multi-site sQTBA approach as an attempt to triangulate identified sources as discussed by other researchers (Brook et al., 2004; Zhao et al., 2007) while simultaneously reducing the impact of trajectory flow characteristics (Keeler and Samson, 1989).

In general, most of the metal species seemed to have temporal trends that did not correspond with observed seasonal variations of $\text{PM}_{2.5}$ (see Table S4 in the SM) indicative of local emissions driven by local dispersion characteristics.

Acknowledgments

The authors gratefully acknowledge the NOAA Air Resources Laboratory (ARL) for the provision of the HYSPLIT transport and dispersion model used in this application. We also thank Clarissa Whitelaw of the Air Quality Monitoring Unit (AQMU), OMOE for logistical support during the period of study. Finally, we thank Andy Ng and Dr. Nick Karellas of the AQMU for the two-year optimization studies of the Xact™ 620 ambient metals monitor.

Supporting Material Available

Time series, CPF, sQTBA, RTWC and scatter plots for up to 16 additional species, supporting tables and discussions can be found

in Figures S1–S73; Tables S1–S4 and Discussions S1–S4 respectively. This information is available free of charge via the internet at <http://www.atmospolres.com>.

References

- Allen, G.A., Babich, P., Poirot, R.L., 2004. Evaluation of a new approach for real-time assessment of woodsmoke PM. *Proceedings of the Regional and Global Perspectives on Haze: Causes, Consequences, and Controversies, Air and Waste Management Association Visibility Specialty Conference*, October 25–29, 2004, Asheville, NC, pp. 16.
- Ashbaugh, L.L., Malm, W.C., Sadeh, W.Z., 1985. A residence time probability analysis of sulfur concentrations at Grand Canyon National Park. *Atmospheric Environment* 19, 1263–1270.
- Bauer, J.J., Yu, X.Y., Cary, R., Laulainen, N., Berkowitz, C., 2009. Characterization of the sunset semi-continuous carbon aerosol analyzer. *Journal of the Air & Waste Management Association* 59, 826–833.
- Begum, B.A., Kim, E., Jeong, C.H., Lee, D.W., Hopke, P.K., 2005. Evaluation of the potential source contribution function using the 2002 Quebec forest fire episode. *Atmospheric Environment* 39, 3719–3724.
- Brereton, C.A., Johnson, M.R., 2012. Identifying sources of fugitive emissions in industrial facilities using trajectory statistical methods. *Atmospheric Environment* 51, 46–55.
- Brook, J.R., Johnson, D., Mamedov, A., 2004. Determination of the source areas contributing to regionally high warm season $\text{PM}_{2.5}$ in eastern North America. *Journal of the Air & Waste Management Association* 54, 1162–1169.

- Cheng, M.D., Hopke, P.K., Barrie, L., Rippe, A., Olson, M., Landsberger, S., 1993a. Qualitative determination of source regions of aerosol in Canadian high Arctic. *Environmental Science & Technology* 27, 2063–2071.
- Cheng, M.D., Hopke, P.K., Zeng, Y.S., 1993b. A receptor-oriented methodology for determining source regions of particulate sulfate observed at Dorset, Ontario. *Journal of Geophysical Research – Atmospheres* 98, 16839–16849.
- Cooper Environmental Services, 2009. XACT™ 620 Technical Documents, Volume I: User's Guide, Portland, Oregon, 16 pages.
- Dabek-Zlotorzynska, E., Dann, T.F., Martinelango, P.K., Celso, V., Brook, J.R., Mathieu, D., Ding, L.Y., Austin, C.C., 2011. Canadian National Air Pollution Surveillance (NAPS) PM_{2.5} speciation program: methodology and PM_{2.5} chemical composition for the years 2003–2008. *Atmospheric Environment* 45, 673–686.
- Draxler, R.R., Rolph, G.D., 2010. http://ready.arl.noaa.gov/HYSPLIT_traj.php, accessed in 2012.
- Environment Canada, 2013a. http://climate.weather.gc.ca/advanceSearch/searchHistoricData_e.html, accessed in 2013.
- Environment Canada, 2013b. <http://www.ec.gc.ca/inrp-npri/default.asp?lang=en&n=0EC58C98->, accessed in 2013.
- Government of Canada, 2009. Proposed Risk Management Approach for C.I. Pigment Yellow 34, Chemical Abstracts Service Registry Number (CAS RN): 1344–37–2, 16 pages.
- Goyer, R., 2004. Issue Paper on the Human Health Effects of Metals, Washington DC, 44 pages.
- Harrison, R.M., Yin, J.X., 2000. Particulate matter in the atmosphere: which particle properties are important for its effects on health? *Science of the Total Environment* 249, 85–101.
- Henry, R.C., 2003. Multivariate receptor modeling by N-dimensional edge detection. *Chemometrics and Intelligent Laboratory Systems* 65, 179–189.
- Hwang, I., Hopke, P.K., 2007. Estimation of source apportionment and potential source locations of PM_{2.5} at a west coastal IMPROVE site. *Atmospheric Environment* 41, 506–518.
- Jeong, C.H., McGuire, M.L., Herod, D., Dann, T., Dabek-Zlotorzynska, E., Wang, D., Ding, L.Y., Celso, V., Mathieu, D., Evans, G., 2011. Receptor model based identification of PM_{2.5} sources in Canadian cities. *Atmospheric Pollution Research* 2, 158–171.
- Jeong, C.H., Hopke, P.K., Kim, E., Lee, D.W., 2004. The comparison between thermal-optical transmittance elemental carbon and Aethalometer black carbon measured at multiple monitoring sites. *Atmospheric Environment* 38, 5193–5204.
- Keeler, G.J., Samson, P.J., 1989. Spatial representativeness of trace-element ratios. *Environmental Science & Technology* 23, 1358–1364.
- Kim, E., Hopke, P.K., Kenski, D.M., Koerber, M., 2005. Sources of fine particles in a rural midwestern U.S. area. *Environmental Science & Technology* 39, 4953–4960.
- Kim, E., Hopke, P.K., Edgerton, E.S., 2003. Source identification of Atlanta aerosol by positive matrix factorization. *Journal of the Air & Waste Management Association* 53, 731–739.
- Neuberger, M., Schimek, M.G., Horak, F., Moshhammer, H., Kundi, M., Frischer, T., Gomiscek, B., Puxbaum, H., Hauck, H., Auphep-Team, 2004. Acute effects of particulate matter on respiratory diseases, symptoms and functions: epidemiological results of the Austrian Project on Health Effects of Particulate Matter (AUPHEP). *Atmospheric Environment* 38, 3971–3981.
- NOAA ARL, 2008. http://www.arl.noaa.gov/faq_hg11.php, accessed in 2013.
- Ogulei, D., Hopke, P.K., Zhou, L.M., Paatero, P., Park, S.S., Ondov, J., 2005. Receptor modeling for multiple time resolved species: the Baltimore, supersite. *Atmospheric Environment* 39, 3751–3762.
- Ondov, J.M., Buckley, T.J., Hopke, P.K., Ogulei, D., Parlange, M.B., Rogge, W.F., Squibb, K.S., Johnston, M.V., Wexler, A.S., 2006. Baltimore supersite: highly time- and size-resolved concentrations of urban PM_{2.5} and its constituents for resolution of sources and immune responses. *Atmospheric Environment* 40, S224–S237.
- Ontario Ministry of the Environment, 2012. Air Quality in Ontario Report for 2010, Ontario, Canada, 90 pages.
- Paatero, P., Hopke, P.K., Begum, B.A., Biswas, S.K., 2005. A graphical diagnostic method for assessing the rotation in factor analytical models of atmospheric pollution. *Atmospheric Environment* 39, 193–201.
- Pekney, N.J., Davidson, C.I., Zhou, L.M., Hopke, P.K., 2006. Application of PSCF and CPF to PMF-modeled sources of PM_{2.5} in Pittsburgh. *Aerosol Science and Technology* 40, 952–961.
- Pope, C.A., Burnett, R.T., Thurston, G.D., Thun, M.J., Calle, E.E., Krewski, D., Godleski, J.J., 2004. Cardiovascular mortality and long-term exposure to particulate air pollution – epidemiological evidence of general pathophysiological pathways of disease. *Circulation* 109, 71–77.
- Rastogi, A.K. 2013. <http://code.google.com/p/metcor/>, accessed in 2013.
- Rizzo, M.J., Scheff, P.A., 2007. Fine particulate source apportionment using data from the USEPA speciation trends network in Chicago, Illinois: comparison of two source apportionment models. *Atmospheric Environment* 41, 6276–6288.
- Seibert, P., Kromp-Kolb, H., Baltensperger, U., Jost, D.T., Schwikowski, M., Kasper, A., Puxbaum, H., 1994. Trajectory analysis of aerosol measurements at high alpine sites, in *Transport and Transformation of Pollutants in the Troposphere*, edited by Borrell, P.M., Borrell, P., Cvitas, T., Seiler, W., Academic Publishing, Den Haag, pp. 689–693.
- Sofowote, U.M., Hung, H., Rastogi, A.K., Westgate, J.N., Deluca, P.F., Su, Y.S., McCarry, B.E., 2011. Assessing the long-range transport of PAH to a sub-Arctic site using positive matrix factorization and potential source contribution function. *Atmospheric Environment* 45, 967–976.
- Stohl, A., 1998. Computation, accuracy and applications of trajectories – a review and bibliography. *Atmospheric Environment* 32, 947–966.
- Stohl, A., 1996. Trajectory statistics – a new method to establish source-receptor relationships of air pollutants and its application to the transport of particulate sulfate in Europe. *Atmospheric Environment* 30, 579–587.
- Stohl, A., Seibert, P., 1998. Accuracy of trajectories as determined from the conservation of meteorological tracers. *Quarterly Journal of the Royal Meteorological Society* 124, 1465–1484.
- Sunder Raman, R., Hopke, P.K., 2007. Source apportionment of fine particles utilizing partially speciated carbonaceous aerosol data at two rural locations in New York State. *Atmospheric Environment* 41, 7923–7939.
- Thermo Fisher Scientific Inc., 2007. Model 5030, Instruction Manual. Synchronized Hybrid Ambient Real-Time Particulate Monitor, Thermo Fisher Scientific Inc., Air Quality Instruments, Franklin, MA 02038, xvi–124.
- Thurston, G.D., Spengler, J.D., 1985. A quantitative assessment of source contributions to inhalable particulate matter pollution in metropolitan Boston. *Atmospheric Environment* 19, 9–25.
- U.S. EPA (U.S. Environmental Protection Agency), 2013a. www.epa.gov/ttn/airquality/2008inventory.html, accessed in 2013.
- U.S. EPA (U.S. Environmental Protection Agency), 2013b. <http://www.epa.gov/air/emissions/where.htm>, accessed in 2013.
- U.S. EPA (U.S. Environmental Protection Agency), 2011. <http://www.epa.gov/ttn/amt/criteria.html>, accessed in 2012.
- Venier, M., Ma, Y.N., Hites, R.A., 2012. Bromobenzene flame retardants in the great lakes atmosphere. *Environmental Science & Technology* 46, 8653–8660.
- Wang, Y.G., Hopke, P.K., Rattigan, O.V., Chalupa, D.C., Utell, M.J., 2012. Multiple-year black carbon measurements and source apportionment using delta-C in Rochester, New York. *Journal of the Air & Waste Management Association* 62, 880–887.
- Wang, Y.G., Hopke, P.K., Rattigan, O.V., Xia, X.Y., Chalupa, D.C., Utell, M.J., 2011. Characterization of residential wood combustion particles using the two-wavelength aethalometer. *Environmental Science & Technology* 45, 7387–7393.
- Wang, Y.G., Huang, J.Y., Zhan, T.J., Hopke, P.K., Holsen, T.M., 2010. Impacts of the Canadian forest fires on atmospheric mercury and

- carbonaceous particles in northern New York. *Environmental Science & Technology* 44, 8435–8440.
- Westgate, J.N., Wania, F., 2011. On the construction, comparison, and variability of airsheds for interpreting semivolatile organic compounds in passively sampled air. *Environmental Science & Technology* 45, 8850–8857.
- Wu, C.F., Larson, T.V., Wu, S.Y., Williamson, J., Westberg, H.H., Liu, L.J.S., 2007. Source apportionment of PM_{2.5} and selected hazardous air pollutants in Seattle. *Science of the Total Environment* 386, 42–52.
- Yadav, V., Turner, J., Downs, J., Rowles, T., 2009. High time resolution PM₁₀ metals by the CES ambient metals monitor (Xact 620): Field performance evaluation and data trends for St. Louis. *Proceedings of the 102nd Annual Meeting of the Air & Waste Management Association*, Detroit, MI, 06/16/2009 - 06/19/2009, Detroit, MI.
- Yap, D., Reid, N., DeBrou, G., Bloxam, R., 2005. Transboundary Air Pollution in Ontario, Ontario, Canada, 115 pages.
- Zeng, Y.S., Hopke, P.K., 1994. Comparison of the source locations and seasonal patterns for acidic species in precipitation and ambient particles in southern Ontario, Canada. *Science of the Total Environment* 143, 245–260.
- Zeng, Y., Hopke, P.K., 1989. A study of the sources of acid precipitation in Ontario, Canada. *Atmospheric Environment* 23, 1499–1509.
- Zhao, W.X., Hopke, P.K., Zhou, L.M., 2007. Spatial distribution of source locations for particulate nitrate and sulfate in the upper–midwestern United States. *Atmospheric Environment* 41, 1831–1847.
- Zhou, L.M., Hopke, P.K., Liu, W., 2004a. Comparison of two trajectory based models for locating particle sources for two rural New York sites. *Atmospheric Environment* 38, 1955–1963.
- Zhou, L.M., Hopke, P.K., Paatero, P., Ondov, J.M., Pancras, J.P., Pekney, N.J., Davidson, C.I., 2004b. Advanced factor analysis for multiple time resolution aerosol composition data. *Atmospheric Environment* 38, 4909–4920.